LONGITUDINAL DYNAMICS IN AN FFAG ACCELERATOR UNDER CONDITIONS OF RAPID ACCELERATION AND FIXED, HIGH RF

S. Koscielniak*, TRIUMF, Vancouver, B.C., Canada
C. Johnstone, FNAL, Batavia, IL 60510, USA

Abstract

A signature of fixed-field acceleration is that the orbit of the beam centroid unavoidably changes with energy. The corresponding change in pathlength results in phase slip relative to the fixed-frequency accelerating waveform. Nevertheless, depending on the location of the fixed-points of the motion, synchronous or asynchronous cross-crest acceleration is possible for a limited number of turns. The possibility of asynchronous rf can be understood simply by realizing that for acceleration in a single pass, the initial cavity phases can be set to exactly compensate for the phase slip. The present work explores the influence of the path-length fixed points and of rf manipulations on the longitudinal dynamics in FFAGs.

INTRODUCTION

In a regime where acceleration is completed in a few turns or tens of turns, cost/technology constraints imply that both the magnetic field and the radio frequency are fixed and that the particle beam transits the radial aperture during acceleration. The fastest acceleration and the most effective use of voltage arises during on- or cross- crest operation. If one abandons the constraint of isochronous orbits, as is inevitable for highly-relativistic beams, there is much range for creativity in design of the magnet lattice and the phase-slip profile. However, simplifying concepts such as rf buckets and phase stability, etc., no longer apply.

A very important feature of fast acceleration is the freedom to cross betatron resonances. In a non-scaling Fixed-Field Alternating Gradient (FFAG) accelerator, the optics change slowly with energy, crossing resonance tunes, and the orbit pathlength is parabolic as a function of energy. Variable optics allow the machine lattice to be built from linear magnetic elements only with a corresponding large dynamic aperture. The nonscaling FFAG is of particular interest because it provides an opportunity to consider the nature and location of fixed points of a strong nonlinear oscillator as the model for the longitudinal dynamics.

DIFFERENCE EQUATIONS

On the "central orbit" accelerating cavities are spaced a distance L_0 apart and are driven at angular frequency ω with peak voltage V. In the ultra-relativistic limit, non-isochronism results only from path length dependence on energy $\Delta L(E)$. We define $T_0 = L_0/c$ and $\Delta T = \Delta L/c$ with the speed of light c. Let the iteration index be n. We introduce a relative time coordinate $T_n = t_n - nT_s$ where $T_s = 2m\pi/\omega$ and $m = \mathrm{Integer}[\omega T_0/2\pi]$. In the moving frame, the energy E and arrival times are

$$\begin{aligned} E_{n+1} &= E_n + eV\cos(\omega T_n) \\ T_{n+1} &= T_n + \Delta T(E_{n+1}) + (T_0 - T_s)\ . \end{aligned} \quad (1)$$

In the *synchronous* case L_0 is the only free variable; apart from the choice of a harmonic number, ω (and hence T_s) is determined uniquely from L_0. In the *asynchronous* case both L_0 and ω retain the status of free variables.

Realistic equations

Equations (1) are *toy* equations. They apply either to a linac of indefinite length, or to the interaction with a single cavity in a cyclic accelerator. However, the condition of periodicity in a cyclic accelerator (equipped with a string of cavities) alloyed with near-sychronism allows for greater sophistication in the choices for the rf.

Let $\omega T_s = (2m+q)\pi$ where m is an integer and q is a fraction. Let the N_c cavities each have some initial phasing ϕ_n on the first turn. The energy increment is $\propto \cos[\omega T_n\ + (nq\pi + \phi_n)]$. If we set $\phi_n = -nq\pi$ then the simple form of equation (1) is recovered. At the end of the first turn, the beam starts to return through the same cavities a second time. Maintaining synchronism has two consequences. Firstly, for the continued cancellation between $(N_c + k)q\pi$ and ϕ_k it follows that $N_c q = 2M$ with integer $M = 0, 1, 2, \ldots$. Secondly, if one is to avoid a jumping of the phase between turns then $\mathrm{Modulo}[N_c\delta\phi, 2\pi] \approx \delta\phi = \omega(T_0 - T_s)$.

In the *synchronous* case with zero inter-turn phase jumps these conditions lead to a discrete set of frequencies ω. The usual condition is to set $T_s = T_0$. Typically the reference energy does not rise linearly, and the reference phase varies in a roughly sinusoidal fashion. This approach has the advantage that phase deviation moduli never exceed $\pi/2$ and negative energy increments are not encountered.

However, it can be advantageous to break the condition of zero inter-turn phase jump, and to loosen the stricture on q and ϕ_k. In this *asynchronous* case, each line ω is broadened into a narrow continuum. Careful choice may narrow the excursions about the crest of the wave and facilitate a reference orbit for which $\cos(\omega T_n + \phi_n) = 1\ \ \forall n\ .$ (2)

Best frequency and initial phases

Suppose acceleration is to be accomplished in two turns. One may fake an exact (2) by (i) setting the fixed radiofre-

*TRIUMF receives federal funding via a contribution agreement through the National Research Council of Canada

quency to the ideal value for the second turn, and (ii) by adjusting the initial phases at injection so that cavity phases are correct during the first-turn passage of the reference particle. When acceleration extends over more than two turns one may hope to share the deviations from (2) more or less equally among the turns by careful choices. This ambition becomes less achievable, the larger is the number of turns N_t. "Best frequency and phases strategy" refers to maximising $\mathcal{S} = \sum_{n=1}^{N_t \times N_c} \cos[\omega T_n^{\rm ref} + \phi_k]$ with respect to ω and ϕ_k under the *assumption* that we attempt to force the reference particle to arrive at $\cos(\phi) = 1$. This is accomplished in a statistical sense; although many terms are close to unity others will deviate. Generally, as the number of turns is increased so the distribution grows until zero or even negative terms appear in the sum $\mathcal{S}$ (i.e. phase deviation moduli exceed $\pi/2$).

INFLUENCE OF FIXED POINTS

To what degree equations (1) are useful for acceleration depends on the nature and location of the sets of first-order fixed points which are the solutions of $E_{n+1} = E_n$ and $T_{n+1} = T_n$. In what follows, we shall describe how the algebraic form $\Delta T(E)$ influences cross-crest acceleration. Manipulation of $\Delta T(E)$ is really a matter for the magnet lattice designer, so part of the discussion is hypothetical.

Synchronous and asynchronous rf are equally valid. However, for examples we adopt the synchronous case because the absence of inter-turn phase-jumps will generate a simpler and more continuous phase space. Nevertheless, the influence of the $T_{n+1} = T_n$ fixed points is equally important to the asynchronous case.

Linear path dependence

In the case of a scaling, radial-sector FFAG, orbits are staggered radially outward as a function of momentum and the orbital change can be approximately linear with energy. For linear path dependence $\Delta T = \alpha(E - E_c)$, equations (1) correspond to motion within a stationary r.f. bucket. E_c is the energy of the central orbit. A beamlet injected at bucket bottom will be accelerated to the bucket top during one half synchrotron oscillation. The beam twice crosses the crest of the voltage waveform; and those moments correspond to the maximal acceleration rate. The minimum voltage occurs when bucket height is set equal to the difference of extraction and injection energies.

Quadratic path dependence

The case of quadratic path length dependence on energy is important since it corresponds to that of the non-scalling FFAG type accelerator, which is considered for rapid acceleration of muons[1, 2, 3]. Figure 1 show the phase space generated by the model equations $y \propto (E - E_c)$ and

$$dy/ds \propto \cos(x\pi/2)\ ,\ dx/ds \propto y^2 - 1\ . \qquad (3)$$

There are two elliptic and two hyperbolic fixed points. There is libration and rotation, as in the linear case, but a striking new feature of the phase space is a serpentine libration that flows along $y = +2, -2, +2, -2, \ldots$ while x increases without limit. This meander feature, emphasised in figure 2, can be used to augment the range of acceleration. A beamlet introduced at $(x, y) = (-1, -2)$ may be later extracted at to $(1, 2)$. Because there are two $T_{n+1} = T_n$ fixed points, there are two reversals of the phase-slip direction. Thi is an advantage because it allows the beam to cross the waveform crest three times before the phase slips to values where the beamlet is decelerated. The width of the meander varies weakly with the voltage.

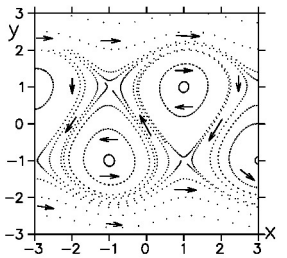

Figure 1: Phase space of quadratic pendulum

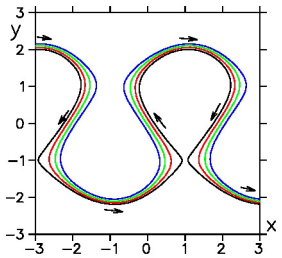

Figure 2: Manifold of serpentine libration

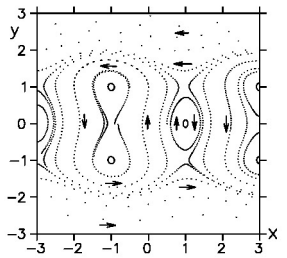

Figure 3: Phase space of cubic pendulum, $\alpha = 1$

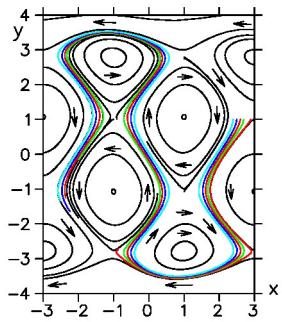

Figure 4: Phase space of quartic pendulum, $\alpha = 1/3$

Cubic path dependence

Consider the model equations:

$$dy/ds \propto \cos(x\pi/2)\ , \qquad dx/ds \propto y(1 - \alpha^2 y^2)\ . \qquad (4)$$

As the cubic parameter α is increased, the $y \neq 0$ fixed points come to dominate the motion. For example $\alpha = 1$ in figure 3. The acceleration range diminishes but some of the phase-space paths become almost vertical which facilitates faster acceleration. Moreover, there are some phase profiles which cross the crest four times which implies more effective use of the accelerating voltage.

Quartic path dependence

Consider the model equations:

$$dy/ds \propto \cos(x\pi/2)\ , \qquad dx/ds \propto y^2(1-\alpha^2 y^2) - 1\ . \qquad (5)$$

As α approaches $\simeq 1/3$, the quartic fixed points (i.e. at large $|y|$) begin to dominate the phase space motion; and a bi-serpentine libration emerges with twice as many manders, as shown in figure 4. The beamlet injected at

$(x, y) = (1, -3.5)$ is extracted at $(-1, 3.5)$. The phase profile crosses the crest of the waveform five times, and the acceleration range is extended to $y = \pm 3.5$. Thus four reversals of phase-slip direction is advantageous; because it allows the beamlet to cross the crest five times before the phase slips to values where deceleration occurs.

From these examples we have seen the general features: (i) number of crest crossings equal to one plus the order of the polynomial, and (ii) meanders only occur for even orders.

PARTICLE TRACKING

As a particular example, we take a non-scaling FFAG of 2 km circumference and path length variation $\Delta L(E)$ up to 50 cm (120° of rf phase). The machine has 300 cells and 200 MHz rf cavities. Particle tracking was completed both for asynchronous and synchronous rf for acceleration completed in a number of turns ranging from two to ten. Figures 5,6 and figs. 7,8 show the beam centroid motion for the asynchronous and synchronous cases, respectively.

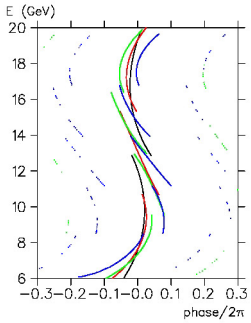

Figure 5: Phase portrait for 2–5 turns acceleration.

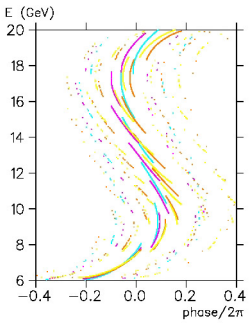

Figure 6: Phase portrait for 6–9 turns acceleration.

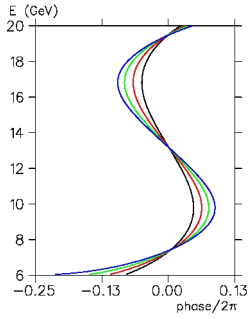

Figure 7: Phase portrait for 3–6 turns acceleration.

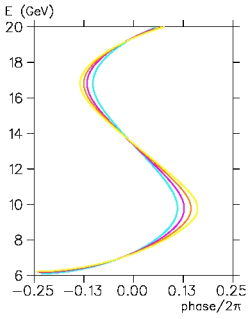

Figure 8: Phase portrait for 7–10 turns acceleration.

Table 1 captures the variation of output emittance with voltage per turn and number of turns. The table is unable to indicate the emittance quality; to what degree the phase space is distorted, whether there are voids or tails, etc. However, an indication of relative quality is given in figures 9,10 and 11,12 for asynchronous and synchronous rf, respectively.

For five or less turns, the output emittance for the asynchronous scheme is superior. For six and seven turns, the emittance quality is comparable for the two schemes. For eight or more turns, the output emittance is superior for the synchronous rf scheme.

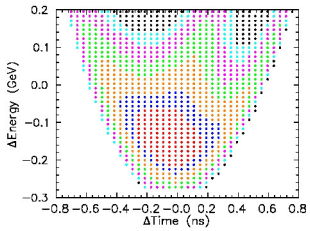

Figure 9: Input emittance

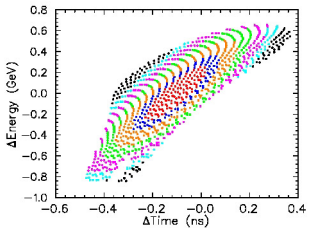

Figure 10: Output emittance

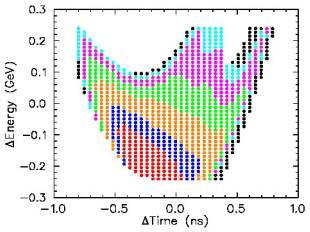

Figure 11: Input emittance

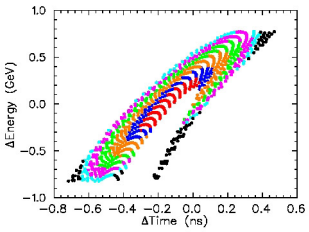

Figure 12: Output emittance

Table 1: Comparative performance

Turns #	over factor	volts GV	emittance eV.s [Asynk]	emittance eV.s [Synk]
4	1.10	3.850	0.2590	0.3150
5	1.15	3.220	0.5114	0.3520
6	1.15	2.683	0.4701	0.4580
7	1.20	2.400	0.4646	0.4518
8	1.25	2.187	0.1479	0.2962
9	1.30	2.022	0.1806	0.2684
10	1.30	1.820	–	0.1017

CONCLUSION

The "fast regime" in a fixed-field accelerator opens a new frontier of beam dynamics in which non-linear pathlength variation with energy and fixed radio-frequency combine to give a longitudinal phase space that is both useful for acceleration and rich in new physics. We have categorized the motion in terms of its fixed points; and we have developed a context for the "best frequency and phases" rf strategy that emphasises the distinction between synchronous and asynchronous rf. Finally, for the quadratic pathlength dependence in a non-scaling FFAG we have compared the relative performance, in identical machines, of synchronous and asynchronous rf schemes.

REFERENCES

[1] C.Johnstone and S.Koscielniak: *Recent Progress on FFAGs For Rapid Acceleration*, proceedings of Snowmass 2001, 30 Jun-21 Jul 2001, Snowmass Village, CO.

[2] J.S. Berg: *Longitudinal Reference Particle Motion in Nearly Isochronous FFAG Recirculating Accelerators*, ibid.

[3] C.Johnstone and S.Koscielniak: *FFAGs for Rapid Acceleration*, accepted for publication NIM-A Nov. 2002.